Cluster-assembled overlayers and high-temperature superconductors

T. R. Ohno, Y.-N. Yang, G. H. Kroll, K. Krause, L. D. Schmidt, and J. H. Weaver
Department of Materials Science and Chemical Engineering, University of Minnesota, Minneapolis, Minnesota 55455

Y. Kimachi and Y. Hidaka
NTT Laboratories, 162 Tokai, Ibaraki, 319-11, Japan

S. H. Pan and A. L. de Lozanne
Department of Physics, University of Texas, Austin, Texas 78712
(Received 23 October 1990)

X-ray photoemission results for interfaces prepared by cluster assembly with nanometer-size clusters deposited on high-T_c superconductors (HTS's) show a reduction in reactivity because atom interactions with the surface are replaced by cluster interactions. Results for conventional atom deposition show the formation of overlayer oxides that are related to oxygen depletion and disruption of the near-surface region of the HTS's. For cluster assembly of Cr and Cu, there is a very thin reacted region on single-crystal $Bi_2Sr_2CaCu_2O_8$. Reduced reactivity is observed for Cr cluster deposition on single-crystal $YBa_2Cu_3O_7$-based interfaces. There is no evidence of chemical modification of the surface for Ge and Au cluster assembly on $Bi_2Sr_2CaCu_2O_8(100)$. The overlayer grown by Au cluster assembly on $Bi_2Sr_2CaCu_2O_8$ covers the surface at low temperature but roughening occurs upon warming to 300 K. Scanning-tunneling-microscopy results for the Au(cluster)/$Bi_2Sr_2CaCu_2O_8$ system warmed to 300 K shows individual clusters that have coalesced into large clusters. These results offer insight into the role of surface energies and cluster interactions in determining the overlayer morphology. Transmission-electron-microscopy results for Cu cluster assembly on silica show isolated irregularly shaped clusters that do not interact at low coverage. Sintering and labyrinth formation is observed at intermediate coverage and, ultimately, a continuous film is achieved at high coverage. Silica surface wetting by Cu clusters demonstrates that dispersive force are important for these small clusters.

I. INTRODUCTION

The effects of intermixing caused by chemical reactions for interfaces between the high-temperature superconductors (HTS's) and other materials are important in HTS device applications and studies of such fundamental properties as the superconducting gap. Many studies have focused on basic chemical interactions at interfaces formed by the deposition of overlayers *in vacuo* onto single-crystal and polycrystalline HTS surfaces.[1] Adatom condensation has been shown to result in chemical changes and structural disruption of the HTS surface region for a wide variety of overlayer materials.[1–10] In most cases, interface reactivity can be related to the extraction of oxygen from relatively weak Cu-O planar structures as more favorable overlayer oxides are formed.[1–12] Such complex, largely uncharacterized interface morphologies are not advantageous for basic or applied studies of HTS's that presume simple boundary layers.

It has been shown recently that overlayers can be formed by cluster assembly, i.e., deposition of clusters containing tens to thousands of atoms onto a surface. These clusters are preformed by atom deposition and nucleation on a condensed Xe layer at 20 K. Cluster deposition is accomplished by subliming the Xe at $\sim$100 K, lowering the clusters to the substrate. One of the advantages of this growth process is that it changes the kinetic pathways at the surface enough to produce undisrupted interfaces.[13] This growth technique offers the possibility of examining HTS interfaces with little or no modification of the superconducting surface region. In addition, the relevance of macroscopic quantities such as surface energies and heats of oxide formation can be addressed for small clusters where van der Waals forces may play an important role.

In this paper we examine several cluster-assembled HTS interfaces, focusing on issues related to surface structure, surface chemistry, and reaction mechanisms. Insight into the structure of overlayers on these HTS surfaces is given by transmission electron microscopy (TEM) for Cu clusters deposited on silica substrates. Additional insight into overlayer structure is obtained from scanning-tunneling-microscopy (STM) images of a Au-assembled layer on $Bi_2Sr_2CaCu_2O_8(100)$. The full range of cluster reactivity with the HTS's is explored with x-ray photoemission spectroscopy (XPS) by considering Cr, Ge, Cu, and Au overlayers. The tendency of atom-deposited Au and Cr layers to form three-dimensional islands in accordance with energy minimization was also observed with the cluster-assembled layers. In contrast, Ge formed a uniform layer when deposited as atoms or clus-

ters. Cu cluster assembly on $Bi_2Sr_2CaCu_2O_8$ resulted in a more extended reacted region at low temperature than observed for Cr, an overlayer expected to be very reactive. Finally, results for cluster assembly on $YBa_2Cu_3O_7(100)$ show that this HTS surface is much less stable than $Bi_2Sr_2CaCu_2O_8$. At the same time, cluster assembly for $YBa_2Cu_3O_7$ is much less disruptive than atom assembly.

II. EXPERIMENTAL TECHNIQUES

Most of the experiments were conducted in an ultrahigh-vacuum (UHV) system with a sample preparation chamber attached via a gate valve to an analysis chamber (base pressure 6×10^{-11} Torr). The latter housed a high-resolution, small-spot x-ray photoelectron spectrometer. A monochromatized Al $K\alpha$ beam ($h\nu=1486.6$ eV) was focused to a 300-μm spot on the sample, and the photoelectrons were energy-analyzed with a hemispherical analyzer (acceptance angle 30°) and a position-sensitive resistive anode. The overall resolution was 0.7 eV at a pass energy of 50 eV and 300-μm spot size, as determined by the width of the Fermi edge for a gold standard. Samples were anchored to the cold head of a closed-cycle He refrigerator using an *in situ* Ga soldering procedure that allows sample interchange without compromising base temperature or pressure.[14] Stable temperatures between 20 and 350 K were accessible using a heater to counteract the refrigerator. Temperatures were measured with a Au-Fe/Chromel thermocouple located near the sample. In other studies, we have noted that condensed O_2 and Ar rapidly desorbed 10 K above the lowest temperature attained, while Xe multilayers were removed by an additional 20 K. From reported vapor pressures for condensed gases, we estimated our minimum temperature to be 20 K.[15] Since the rigidly attached samples had irregularly cleaved surfaces, the average takeoff angle was determined by measuring the attenuation of the substrate emission for a series of Xe exposures, with comparison to mean free paths determined for Xe layers on mirrorlike GaAs(110) cleaved surfaces. Areas used had measured average takeoff angles between 30° and 50°.

Single crystals of $YBa_2Cu_3O_7$ were grown from a melt containing Y_2O_3, $BaCO_3$, and CuO powders in a 0.095 : 0.238 : 0.667 molecular ratio, the melt was heated to 1570 K for 4 h before cooling slowly to room temperature.[16] After annealing in an oxygen flow at 820 K for 200 h, the samples showed superconducting transitions that began at 93 K and reached zero resistivity at 90 K. The $YBa_2Cu_3O_7$ samples were approximately $3\times2\times0.2$ mm^3 in size. A melt containing CaO, $SrCO_3$, Bi_2O_3, and CuO was used to grow $Bi_2Sr_2CaCu_2O_8$ single crystals. These samples were typically $6\times4\times1$ mm^3 in size. The superconducting transition temperature of the $Bi_2Sr_2CaCu_2O_8$ samples was 84 K and the transition width was 3 K. Details concerning the samples can be found in Ref. 16. Clean surfaces were obtained by mounting the crystals onto a rigid post and removing the top surface by prying off a rod epoxied to the sample. Typical cleaved $YBa_2Cu_3O_7$ surfaces were flat and smooth but they had irregular pits that were visible under an optical microscope. The cleaved $Bi_2Sr_2CaCu_2O_8$ surfaces had flat, mirrorlike regions a few mm in size but they also had rough fractured regions. While the use of single-crystal substrates was important because issues related to grain boundaries were avoided, it is important to recognize that even single crystals can contain inclusions and contamination.[1] For our experiments, areas were selected that were flat and had minimum amounts of contamination, based on analysis of the O 1*s* spectra.

The overlayers were grown under identical conditions, and they were examined *in situ* with XPS. For the TEM measurements, the samples were exposed to the atmosphere during transfer to the microscope. TEM bright-field images were obtained with a Philips CM30 scanning transmission-electron microscope (STEM) with 300-keV electrons. The TEM substrates were prepared by depositing ~200 Å of Si onto a Formvar film that covered a Au grid. The Formvar was removed and the silicon was oxidized to an amorphous oxide by heating in an oxygen atmosphere at 920 K for 36 h. The grids were then sandwiched between Cu sheets attached to the HTS sample holder to ensure good thermal contact.

For the STM experiments, the $Bi_2Sr_2CaCu_2O_8$ sample was epoxied to a thin Cu substrate and a Ag-based epoxy was painted along its edge for electrical contact. After cleaving and cluster assembly in UHV, the sample was transferred to a portable vacuum system. Ultimately, it was exposed to the atmosphere for ~10 min during transfer to a low-temperature ultrahigh-vacuum STM. Images were obtained with Pt-Ir (90:10) tunneling tips at 80 K in a constant-current mode (current 100 pA). Tip bias voltages of -1 to -15 V were required to prevent the tip from contacting the sample.

For cluster assembly, depositions were done onto 50-Å-thick Xe buffer layers that were condensed on the HTS surfaces at 20 K. The overlayer materials were evaporated from outgassed, resistively heated sources ~50 cm from the sample at pressures $<3\times10^{-10}$ Torr. The amount deposited was monitored with a quartz-crystal microbalance near the sample. Angstrom units will be used here since the clusters are sufficiently large to have the bulk density. Photoemission studies of the clusters on the Xe layer showed that they were fully metallic, based on the development of bulk valence bands. Such observations have been discussed previously.[13] Heating to ~100 K desorbed the Xe buffer layers and allowed the clusters to come into contact with the pristine HTS surface.

In the following, we will examine changes in substrate core-level line shapes and photoemission intensities as a function of the amount of material deposited. For cluster deposition, the measured substrate photoelectron emission was derived from areas under the clusters and from areas that remained exposed. During overlayer growth, the amount of covered surface increased, and this insured that the core-level line shapes increasingly reflected interfacial effects. Thick overlayers were grown by repeating the cluster deposition process several times.

Information concerning the morphology of the cluster-assembled layers can be obtained by examining the rate at which the substrate emission was attenuated.

Since cluster assembly results in a microscopically irregular surface, the rate of attenuation is slower than would be observed for the same amount of material distributed in a uniform layer. This deviation reflects clusters with dimensions greater than the mean free path of the photoelectron, with the discrepancy dependent on the cluster shape. Such intensity analyses have been discussed by Waddill *et al.*[13] in their synchrotron-photoemission investigation of clusters with various size distributions. They used a model based on uniformly shaped hemispheres to estimate the cluster diameter as a function of the amount of material deposited. For a deposition of 2 Å, the cluster diameter was estimated to be ~30 Å so that a representative cluster contained ~500 atoms. Here, the inelastic mean free paths are larger (10–40 Å) since $h\nu = 1486.6$ eV but the shallower takeoff angle reduces the probed depth by $\sim\frac{1}{2}$. We note that the attenuation is approximately exponential if the cluster thickness is much less than the mean free path so that the rate is approximately that for uniform layer growth.

III. RESULTS AND DISCUSSION

A. Transmission-electron-microscopy results for cluster assembly

To develop an idea of the morphology obtained by cluster assembly on the HTS surface, we deposited Cu clusters onto silica layers supported by conducting Au grids. These samples were examined with TEM after being warmed to 300 K and transferred from the XPS chamber to the electron microscope. The upper panel of Fig. 1 shows a TEM image for 2-Å Cu(clusters) on silica where irregularly shaped features cover ~25% of the surface. A few clusters appear elongated, probably because two or more joined during the deposition process. If we approximate the individual clusters as circular, then the cluster-size-distribution peaks at ~45-Å diam and most have diameters between 35 and 55 Å. A 45-Å-diam cluster would have an average thickness of 8 Å and would contain 750–1000 atoms, based on bulk Cu density, the measured surface coverage, and the 2 Å deposited. Variations in thickness are probably similar to the spread observed in cluster diameter as the contrast between clusters does not indicate large differences. This size is in good agreement with the estimates of Waddill *et al.*[13] based on their photoemission-attenuation analyses. The typical spacing between clusters is ~40 Å, with some separated by as little as ~10 Å. The isolated clusters show little apparent motion, even at room temperature, since there is no evidence of significant coalescence for 2-Å cluster deposition.

These results suggest that surface wetting occurs for Cu clusters on silica, resulting in thin flattened-disk shapes. Observations of Cu films grown by atom deposition on silica substrates at 300 K and higher temperatures have shown a tendency to ball up, even when the films are 500–5000 Å thick. This is a result of the low-substrate surface energy and the absence of strong bonding of Cu to silica.[17,18] Indeed, the surface free energy of Cu and thin amorphous SiO_x are 1.8 and 0.06 J/m^2, respectively,[19,20] and the interfacial energy of Cu and SiO_2 is approximately 1.0–1.5 J/m^2, based on other metal-oxide energies.[21] (By way of reference, 1 J/m^2 corresponds to ~0.6 eV/atom for a surface with planar density of 1×10^{15} atoms/cm^2; this is a typical surface density.) This results in clusters that do not wet the silica, according to Young's formulation of wetting angles. However, for clusters in our size range of tens of angstroms, the long-range van der Waals (dispersion) forces must be considered in the expression of the contact angle.[22,23] (A discussion of the nature of these forces is beyond the scope of this paper, but see Ref. 24. Moreover, they are generally unknown on these small-length scales. We note only that they can be attractive or repulsive, as determined by the frequency dependencies of the polarizability of the media involved.) Wetting of the Cu clusters here suggests that an attractive dispersion force exists. The strength of the force, which is expressed classically by the Lifshitz–van der Waals constant,[25] is similar for most

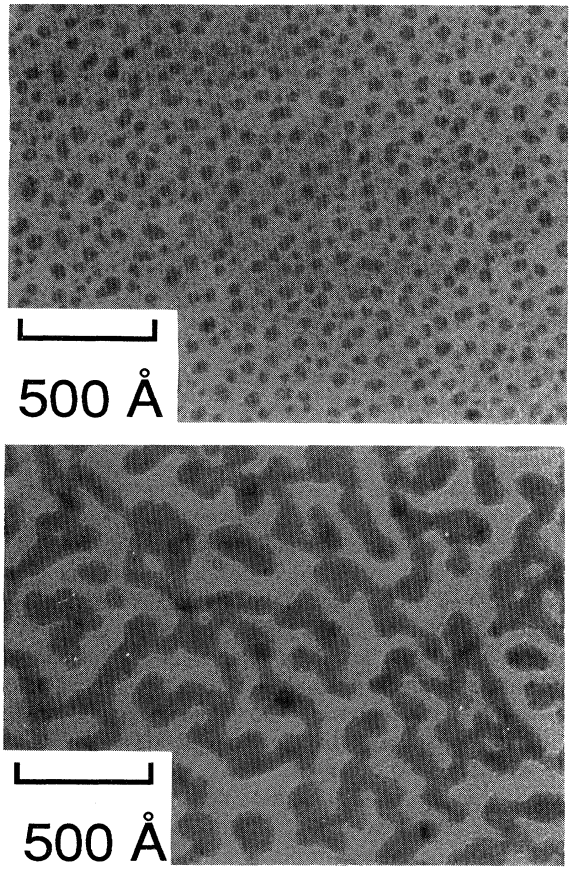

FIG. 1. TEM images of Cu cluster assembly on silica. The upper panel for 2-Å deposition shows irregular clusters over ~25% of the surface (characteristic diameter ~40 Å). The lower panel shows the structure obtained by three successive 2-Å cluster depositions. In this case, the interconnected Cu labyrinth covered ~60% of the surface (estimated thickness ~10 Å). The TEM images showed little contrast after ten such cluster depositions.

metals and should reflect such effects in HTS surfaces as well.

In the absence of cluster-cluster interactions on the substrate, one would expect the surface to be covered in a Poisson-like distribution because cluster deposition is a random process, as is conventional atom deposition. For atom deposition, growth shapes and structures reflect substrate bonding, adatom-adatom bonding, and surface stability. For clusters, the growth structures are again subject to a balance between kinetics and the specifics of cluster-substrate and cluster-cluster interactions. Here, we could examine the interaction of clusters by investigating their spacing on the silica substrate by repeating the cluster deposition process, i.e., depositing clusters onto surfaces already decorated by clusters. For assembly by three consecutive depositions of clusters formed by 2-Å Cu on Xe, the morphology represents a labyrinth, as shown by the lower image of Fig. 1. Elongated metallic lines are clearly visible with contrast that indicates variations in thickness around an average that we estimate to be ~ 10 Å, based on the total amount deposited and the surface coverage of $\sim 60\%$. Although a few of the lines are isolated, most form part of a connected matrix. At the same time, there are open connected areas over 100 Å in size.

Patterns similar to those of Fig. 1 have been observed in the sintering of large particles[26] and in the formation of thin films on weakly interacting interfaces.[18] A liquid-like coalescence model has been used to explain the apparent movement of clusters. In classical sintering theory, the contact of two clusters results in the formation of a neck, as material is transferred primarily via surface diffusion. To reduce the total free energy, the neck broadens, thereby eliminating surfaces of high curvature and causing a net inward movement of the individual cluster centers. The formation of serpentine patterns, however, cannot be accounted for by two-cluster sintering. Instead, rotations resulting from surface-energy anisotropies, multiple-cluster interactions, and cluster-shape irregularities must occur to form the larger open areas observed.[26,27] The observation of small enclosed areas within the Cu pattern demonstrates that nanocluster sintering may create voids similar to the pores observed in classical sintering.

The twisting network of connected clusters shown in Fig. 1 is not observed when the deposition process is repeated in 2-Å increments to a total of 20 Å (not shown). Instead, a relatively uniform contrast in TEM suggests a more homogeneous layer. From these results, we conclude that cluster assembly with small clusters formed on Xe will cover more than half of the surface after three depositions and all of the surface after ten depositions. The complete coverage of the surface is important for interpretation of the interface photoemission results (and Schottky barriers for metal-semiconductor interfaces[13]).

In the following, we will take heed of the results for Cu(clusters) on silica when discussing Au, Ge, Cr, and Cu cluster assembly on $Bi_2Sr_2CaCu_2O_8(100)$ and $YBa_2Cu_2O_7(100)$. At the same time, differences should be expected, and some will be noted. These differences reflect the fact that interaction with the substrate is not identical to that for (chemically inert) silica. In addition, the van der Waals interaction may be different for the HTS's, which are metallic and have different forms for the dielectric function $\epsilon(\omega)$. Given the relative stability of $Bi_2Sr_2CaCu_2O_8$, however, and the fact that the cleaved surface is terminated by a layer of Bi-O, the analogy with silica is reasonable. It is not so reasonable for $YBa_2Cu_3O_7$, and we will present evident for surfaces modified by Cr clusters.

B. Cluster assembly of Au on $Bi_2Sr_2CaCu_2O_8(100)$: Weak substrate interactions

Several previous studies[1] have focused on surface properties for $Bi_2Sr_2CaCu_2O_8$ samples cleaved *in vacuo* and studied at 300 K, and there is general agreement as to the XPS signatures of the clean surface. Here, we have used XPS to establish the spectroscopic baseline for the $Bi_2Sr_2CaCu_2O_8(100)$ surfaces used for cluster assembly. This was done at 300 and 20 K. We found no significant changes in the spectra as a function of temperature (resolution ~ 0.7 eV) that would reflect surface degradation due to oxygen loss or spontaneous surface deterioration.[1] These clean-surface energy distribution curves (EDC's) are shown in the figures to be discussed later in conjunction with interface spectra. Briefly, the clean-surface EDC's show the Cu $2p_{3/2}$ core-level emission consisted of a broad main line at ~ 933 eV and a satellite centered at ~ 942 eV, characteristic of Cu^{2+} bonding in CuO-based HTS materials. The ratio of the Cu $2p_{3/2}$ satellite relative to the main-line intensity was 0.42, and the full width at half maximum (FWHM) of the main line was ~ 4.2 eV. The O 1*s* core level was centered at 528.8 eV and was derived from inequivalent O sites in the unit cell, shifted slightly in energy from one another.[28] In addition, the O spectra showed a contribution amounting to 5–10 % of the total intensity in a feature at ~ 531 eV that has been attributed to an impurity phase.[1] For our purposes, we simply note that it exists and refer the reader to discussions elsewhere.[1,25] The amount of carbon was less than 5% for any $Bi_2Sr_2CaCu_2O_8$ cleaved surface, and there was not significant increase during the experiment due to condensation from residual gases.

Previous results for Au atom deposition on polycrystalline $YBa_2Cu_3O_7$, $La_{1.85}Sr_{0.15}CuO_4$, and $Bi_2Sr_2CaCu_2O_8$ have shown the formation of nonreactive layers, with no evidence for disruption due to adatom condensation.[7–9] These results have also indicated that Au forms clusters at low coverage. The absence of surface reaction and the tendency for clustering are indicative of weak interaction with the HTS surface.

Our experiments involving Au cluster assembly on $Bi_2Sr_2CaCu_2O_8$ followed the procedures outlined above with cleaving at 20 K, the formation of a buffer layer, the deposition of 2-Å Au onto the buffer, and then warming to ~ 100 K to remove the buffer. Data acquisition was done after the sample cooled to 20 K. As expected, the Au clusters were metallic for 2-Å assembly,[13] and the Au emission showed bulk characteristics with the Au $4f_{7/2}$ emission at 83.9 eV. The EDC's for Au (clusters) on $Bi_2Sr_2CaCu_2O_8$ are not shown because the overlayer and

substrate core-level spectra did not change at any coverage for assembly from 2 to 20 Å. We conclude that the Au clusters did not react with the substrate. In drawing this conclusion, it is important to note that the clusters were sufficiently thin that the substrate could be seen and chemical changes could have been detected. Analysis of substrate emission intensity at low temperature showed a nearly exponential attenuation as a function of deposition. As proposed earlier, the simplest model for Au(clusters) on $Bi_2Sr_2CaCu_2O_8$ would be clusters thinner than the photoelectron attenuation length, growing in a fashion analogous to that of Fig. 1. The clusters then ap-

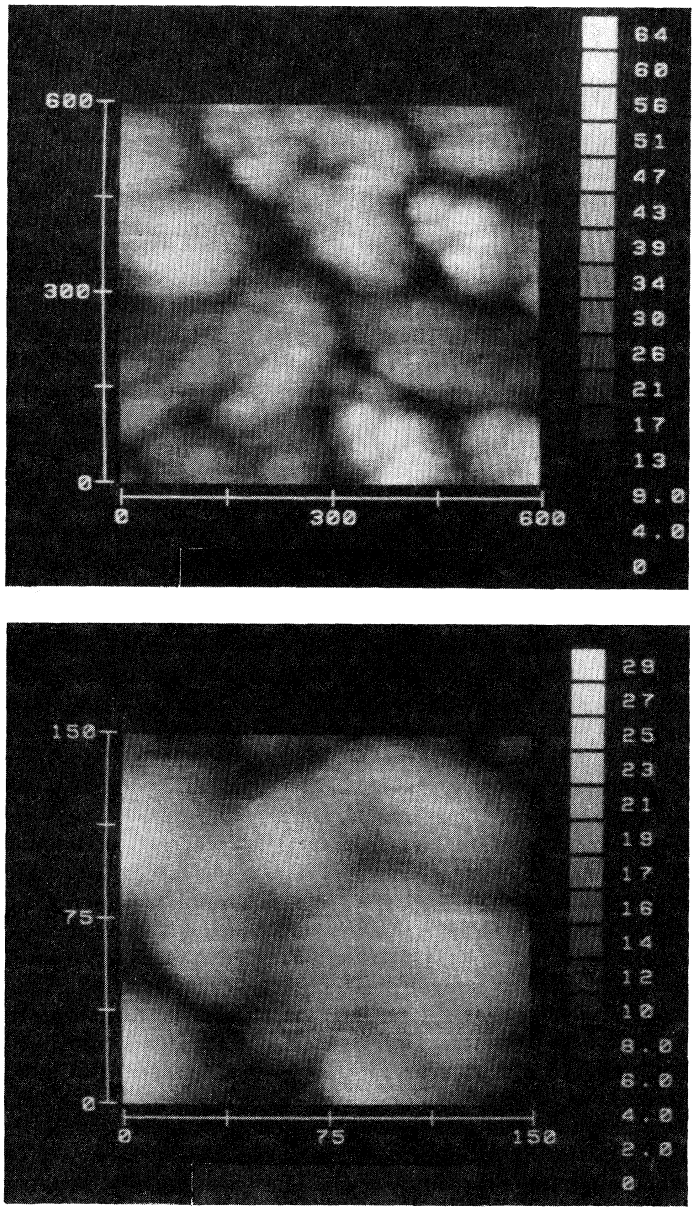

FIG. 2. STM images for 20-Å Au cluster assembly on $Bi_2Sr_2CaCu_2O_8(100)$ after warming to 300 K and a brief air exposure. The upper image for a 600×600-Å^2 region taken with a -15-V tip bias and 100-pA tunneling current shows coarse patches with a typical dimension of ~150 Å and covering $\sim80\%$ of the surface. The dark regions reflect voids formed by cluster coalescence and delamination from the HTS surface. The lower image for a 150×150-Å^2 area (-1 V, 100 pA) shows a single patch that resembles an aggregate composed of smaller clusters of characteristic dimension ~30 Å. The calibrated gray scales on the right-hand side give an indication of height in Å.

peared to wet the surface and probably formed connected patterns with sintering when clusters made contact. We speculate that the 20-Å Au(clusters) on $Bi_2Sr_2CaCu_2O_8$ interface is composed of a large number of small crystallites. However, since assembly was done at ~100 K, the structure also reflects kinetic constraints. (Growth in a fashion approaching thermodynamic equilibrium is more likely for atom deposition; Au atom deposition at 300 K produces large Au clusters that decorate the surface because of the mobility of the adatoms.)

To investigate the stability of the 20-Å Au(clusters) on $Bi_2Sr_2CaCu_2O_8$ interface, we warmed the sample to 300 K *in situ*. There were no changes in the Au $4f$ line shape, and the changes in the substrate line shape were small (the Bi $4f$ EDC's broadened 0.1 eV, but there were no changes in the Cu $2p_{3/2}$ satellite-to-main-line ratio). Although minimal chemical modification occurred, there were clear changes in the morphology of the overlayer. In particular, the Au $4f$ intensity decreased ~10% and the Bi $4f$ and O $1s$ intensities increased 50–80%. This suggests a delamination of the Au layer from the HTS surface to reduce the total surface energy γ of the Au [$\gamma_{Au}=1.5$ J/m^2 (Ref. 20)].

Additional insight into the structural changes for 20-Å Au(clusters) on $Bi_2Sr_2CaCu_2O_8$ warmed to 300 K was obtained from the STM images of Fig. 2. These images were obtained at 80 K for a sample exposed briefly to atmosphere during transfer from the portable vacuum vessel to the UHV STM. The upper panel shows that most of the surface was covered by large patches. The appearance of the patches suggests aggregation of smaller components into bunches in contact with others. The typical dimensions of the aggregates are 100–150 Å. The packing of these irregular shapes resulted in depressions that comprised 10–20% of the total area for different sections examined. Structure within these depressions was not resolvable. The dark areas may correspond to HTS surface regions exposed by the coalescence of the cluster-assembled layer. This is consistent with estimates based on changes observed in substrate photoemission intensities. The aggregates appear to have a moundlike structure, with the highest points reaching <50 Å, and with a much smaller average height. This upper limit is in reasonable agreement with the nominal 20-Å deposition, which would result in an average height of ~25 Å since the surface coverage was reduced. The height is less than other aggregate dimensions, showing that the HTS substrate continued to be wet by the Au at 300 K.

The lower panel of Fig. 2 shows an image of an aggregate with boundaries that result from the attachment of smaller ~30-Å diam clusters. The individual cluster sizes are consistent with those we expect to have formed on the Xe buffer. Sintering to form aggregates when smaller clusters come into contact during growth is energetically favorable, as surface area is reduced. In turn, the energy released upon sintering facilitates atom rearrangement in these nanoscale particles. Warming to 300 K further enhances aggregate growth because of enhanced surface diffusion on the substrate and on the Au clusters. Indeed, recent STM experiments have shown Au atom diffusion on Au over several lattice spacings per sec at 300 K.[29] The STM images of Fig. 2 show that the overlayer retains its cluster-bonded-to-cluster form, even at 300 K, and this assures polycrystalline character rather than the growth of very large crystallites. We note that cross-sectional TEM studies have imaged the lattice planes of a large composite Au cluster on GaAs, showing distinct crystallites.[13]

From these results, it is evident that Au cluster assembly at low temperature produces an overlayer that interacts weakly with the rather inert Bi-O-terminated surface. Cluster-substrate van der Waals interactions result in wetting, as for Cu clusters on silica, but kinetic factors trap the system in a metastable configuration at low temperature. Upon warming to 300 K, the clusters tend to delaminate and structures appear that have smaller surface areas, as shown by the STM images. These results can be understood in terms of the competition between equilibrium thermodynamic growth structures (in this case clusters of Au because of surface free energy consideration) and low-temperature growth constraints imposed by limited transport and van der Waals attraction. Indeed, it is these constraints on atom motion by assembly with clusters that gives different interface structures, as we shall see in the following for reactive systems.

C. Atom and cluster assembly of Ge on $Bi_2Sr_2CaCu_2O_8$(100)

Cluster assembly and atom deposition with Ge offers the opportunity to investigate a semiconductor-superconductor heterostructure. Previous studies of Si atom deposition on Pb-doped $Bi_2Sr_2CaCu_2O_8$ have shown substrate reaction and Si oxidation during the initial stages of overlayer formation,[6] and we expect reaction for Ge atom deposition as well. Figure 3 shows representative core-level EDC's for such atom deposition of Ge onto $Bi_2Sr_2CaCu_2O_8$(100) at 300 K. The spectra are normalized to constant height to emphasize changes in bonding configurations. The bottom EDC of each set of EDC's (except Ge) is for the clean surface, as discussed above.[1] A Ge $2p_{3/2}$ peak appears at 1219.1 eV below E_F for 1-Å deposition, and a new O $1s$ component develops at ~530.5 eV. By 2-Å deposition, a second Ge $2p_{3/2}$ feature appears at 1217.5 eV and it then grows, as shown, and attenuates the first feature. We attribute this behavior to the initial formation of GeO_2-like bonding configurations at the surface[30] followed by the nucleation of elemental Ge on the GeO_2-like layer. [Note that 2 Å corresponds to 8.88×10^{14} atoms/cm^2, compared to the planar density of $Bi_2Sr_2CaCu_2O_8$(100) of 1.37×10^{15} atoms/cm^2. The complete formation of GeO_2-like bonding for 2-Å Ge would require the equivalent of all the oxygen from the Bi-O plane and oxygen from subsurface layers.]

The Cu $2p_{3/2}$ and Bi $4f$ substrate features are decreased rapidly for the first ~2 Å, while the total O $1s$ is reduced only slightly. The O $1s$ substrate emission broadens and shifts 0.3 eV to higher binding energy with 1-Å Ge deposition, indicating that the HTS bonding configurations are changed in the surface region by O redistribution and outdiffusion. The substrate Bi $4f$ features also shift 0.3 eV and broaden as a new spin-

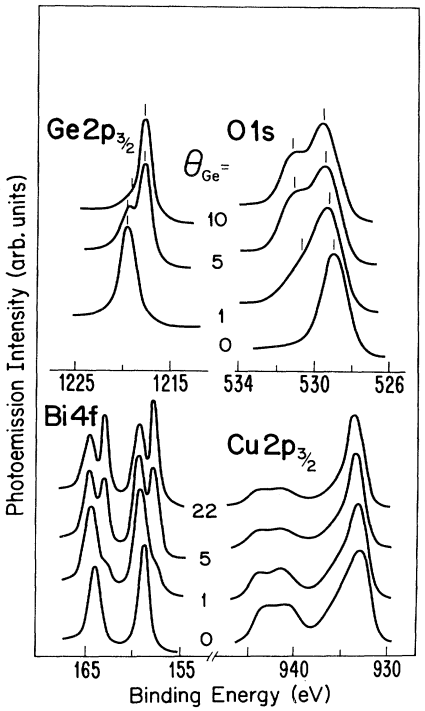

FIG. 3. Core-level EDC's for Ge atom deposition on $Bi_2Sr_2CaCu_2O_8$(100) at 300 K, normalized to constant height to emphasize line-shape changes. For 1-Å deposition, reaction is evident by the GeO_2-like bonding features in the O 1*s* and Ge $2p_{3/2}$ spectra. Bi released from the Bi-O surface plane is evident as the feature that grows at lower binding energy. Changes in the Cu $2p_{3/2}$ results indicate conversion from a valence of +2 to +1. Elemental Ge formed on the reacted region after a 2-Å deposition.

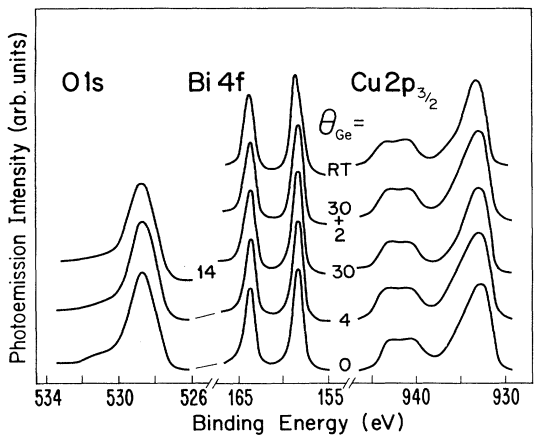

FIG. 4. Core-level EDC's for Ge(clusters) on $Bi_2Sr_2CaCu_2O_8$(100) at low temperature. The Cu $2p_{3/2}$ EDC's are corrected for small contributions from condensed Xe, and a linear background is subtracted. No changes in peak positions or shapes are evident because cluster assembly prevented reactive intermixing. The addition of 2-Å Ge atoms on the cluster-assembled layer does not change the EDC's. Small changes observed when warming to 300 K (RT) reflect limited amounts of cluster HTS reaction at the buried interface.

orbit-split doublet appears at ~1.4-eV lower binding energy. This doublet reflects Bi atoms released by disruption of surface Bi-O planes, as reported for other reacted $Bi_2Sr_2CaCu_2O_8$ interfaces.[1,3–6,10] For ~2-Å Ge atom deposition, the ratio of the Cu $2p_{3/2}$ satellite to the main line also decreases, indicating some disruption of Cu-O planes. There were no significant line-shape changes after 2 Å for Cu and O or for Ge because reaction was largely curtailed by kinetic limitations on oxygen release and transport. Once nucleation of elemental Ge was initiated, the HTS substrate and GeO_2-like emission was attenuated at a rate consistent with approximately uniform overlayer growth, with no indication of the formation of Ge clusters. Thus, Ge appears to wet the GeO_2-like reaction product. In contrast, emission from the released Bi was not attenuated as effectively so that its intensity increased relative to the substrate. This is an indication of segregation rather than trapping in the boundary layers. These observations are then typical of reaction,[1] and they can be used to compare interactions for cluster deposition.

Figure 4 shows normalized core-level EDC's for Ge cluster assembly on $Bi_2Si_2CaCu_2O_8$(100). Assembly was done in 2-Å steps to 20 Å, then in 5-Å steps to 30 Å total. The Ge EDC's showed no changes with coverage, as expected for clusters containing hundreds of atoms. Significantly, there is no indication from the Bi 4*f* and O 1*s* EDC's that changes of the sort observed for Ge atom deposition at 300 K were taking place. For the Cu $2p_{3/2}$ emission, the spectra are distorted by small background changes, and contributions from Xe $M_4N_{4,5}N_{4,5}$ Auger and direct Xe $3p_{3/2}$ emission could be identified. (Xe can recondense since these measurements were done at 20 K. We estimate that ~0.2 ML of Xe recondensed during data acquisition by measuring the Xe $3d_{5/2}$ intensity. It could be removed by warming to ~100 K.) No significant changes are observed in the Cu $2p_{3/2}$ EDC after correction for the adsorbed Xe. As with Au clusters, intensity analysis shows an exponential decrease of the substrate component, indicating a relatively uniform layer derived from thin clusters. This can be seen from the attenuation curves of Fig. 5 where the O and Cu emission intensities are shown normalized to the emission from the clean surface. Finally, to test for exposed areas, we deposited 2 Å of Ge atoms directly onto the 30-Å cluster-assembled interface at low temperature, expecting that these atoms would induce disruption and oxygen withdrawl from exposed surfaces. The results, shown in Fig. 4, indicate no significant changes. We conclude that Ge cluster assembly frustrates the relatively mild reaction observed for Ge atom deposition.

Low-temperature growth may result in a more abrupt interface for Ge clusters because transport processes involving oxygen are constrained. To investigate the chemical stability of the interface, and to determine if delamination occurs, we warmed the (30+2)-Å Ge(clusters) on $Bi_2Sr_2CaCu_2O_8$ interface to 300 K. No changes in the substrate intensities were observed, indicating that the

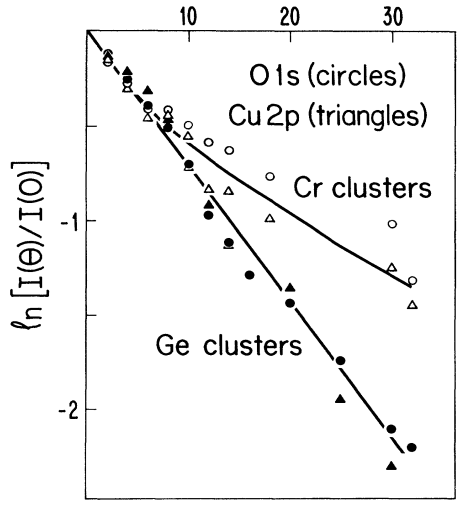

FIG. 5. Attenuation curves for O 1s and Cu $2p_{3/2}$ emission for Ge and Cr cluster deposition onto $Bi_2Sr_2CaCu_2O_8(100)$. Ge clusters yield an exponential attenuation because of simple overlayer growth and wetting of the surface. The nonexponential behavior for Cr clusters reflects a more complex interface structure with Cr cluster agglomeration at the overlayer formation temperature, as driven by the tendency to reduce surface area.

overlayer morphology was not altered in any significant way. The difference between the behavior of the Au and Ge layers can be explained by noting that the surface free energy of Au is 50% greater than Ge. Upon warming, there were changes due to chemical effects at the boundary, as reflected by a 0.2-eV shift and slight broadening of the Bi 4f emission, a 10% reduction of the Cu $2p_{3/2}$ satellite-to-main-line ratio, and a sharpening of the Cu main line. These results indicate intermixing and disruption but on a scale much less than for atom deposition.

A model of the cluster-assembly procedure must explain the stability of the clusters at low temperature, the increased reactivity of the cluster at elevated temperature, and the different final state obtained by this growth method. Atom deposition on a solid HTS surface that contains oxygen can be simply described with a reaction diagram by the separation of the atom from the nearest loosely bound oxygen. For the clean $Bi_2Sr_2CaCu_2O_8$ surface, reaction requires only a small amount of energy to disrupt the surface bonding once the atom is on the surface, and this broadening releases energy. This results in the oxidation of the adatoms, even at 20 K. As the reaction products form, however, they represent a diffusion barrier that must be overcome for further oxidation to occur. This barrier is more easily surmounted at higher temperature and a thicker reaction region forms for atom deposition at 300 K. The reaction pathways are more complex for cluster deposition since the reaction coordinate is not simply the particle separation and the large number of atoms in the cluster results in additional dynamics. When a preformed cluster is deposited at 100 K, the energy released upon bond formation is also reduced since the cluster is already in a lower-energy state than was the free atom. Moreover, there is an activation barrier against intermixing with substrate atoms since any such cluster atom must now be released from the cluster into the interfacial region. At low temperature, thermal activation is insufficient to overcome this barrier and reaction is suppressed. However, when the substrate temperature is increased, dissociation from the cluster is more likely if oxygen is present. The overlayer still differs from that formed by atom deposition at 300 K since the barrier against releasing a cluster atom remains.

D. Atom and cluster assembly of Cr on $Bi_2Sr_2CaCu_2O_8(100)$

The transition-metal elements have shown the greatest reactivity with HTS surfaces for atom deposition because of their high heats of oxide formation. For instance, the heat of formation[31] of Cr_2O_3 ($\Delta H_f = -1128$ kJ/mol) is larger than either GeO_2 or Au_2O_3 ($\Delta H_f = -536.8$ kJ/mol for GeO_2, $\Delta H_f = +81$ kJ/mol for Au_2O_3). The effects can be seen by examining results for Cr atom deposition at 300 K on $Bi_2Sr_2CaCu_2O_8(100)$ summarized in Fig. 6. Again, the lowest EDC's for O, Bi, and Cu are for the clean surface. For 0.25-Å deposition, the Cr $2p_{3/2}$ emission suggests a bonding configuration similar to Cr_2O_3, based on its energy and linewidth.[32] Only 0.25 Å of Cr induces an overall shift in the O 1s emission, and

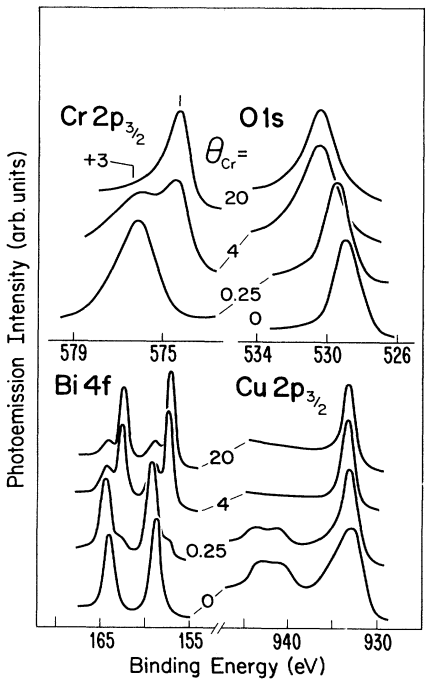

FIG. 6. Core-level EDC's for Cr atom deposition on $Bi_2Sr_2CaCu_2O_8(100)$ at 300 K. By 4-Å Cr atom deposition, effectively all of the Cu atoms within the probed area of ~30 Å have been reduced from +2 to +1 valence due to oxygen loss and surface-region disruption. Line-shape changes for Bi 4f indicate extensive reaction with O from the Bi-O layer and surface segregation of the released Bi atoms.

there is a shoulder at ~531 eV that reflects Cr—O bonding. By 4-Å Cr atom deposition (3.3×10^{15} atoms/cm^2), the nucleation of metallic Cr on the oxide has started, as is evident from the Cr $2p_{3/2}$ emission at 574 eV. Significantly, the Cu $2p_{3/2}$ core-level spectra show complete loss of the satellite by 4 Å as all of the Cu within the probe depth is reduced from formal +2 to +1 valence. Cr atom deposition also induces a shift of 0.3 eV and a broadening of the Bi $4f$ substrate emission because of surface modification. The Cr-induced Bi $4f$ doublet at lower binding energy grows to dominance by 4 Å, indicating substantial redistribution of Bi from disrupted Bi-O planes. Both Bi features were attenuated at the same rate after 6-Å Cr as they were trapped beneath the thickening metal. After 30-Å atom deposition, the Cu $2p_{3/2}$ emission was approximately three times larger than predicted for layer-by-layer growth, and we conclude that Cr grows as three-dimensional clusters on the Cr_2O_3-like layer. Although the consequences in terms of disruption are similar for overlayers of Ge and Cr, the extent of disruption is much greater for Cr.

To investigate Cr cluster assembly on $Bi_2Sr_2CaCu_2O_8$(100), we formed clusters in 2-Å steps up to 14 Å, then in increments of 4 and 12 Å to 30 Å. These clusters were fully metallic at all coverages, based on the Cr $2p_{3/2}$ emission, and there were no changes in Cr $2p_{3/2}$ emission. Representative core-level EDC's for 2 and 30 Å shown in Fig. 7 demonstrate that cluster assembly produces limited $Bi_2Sr_2CaCu_2O_8$ surface changes. Indeed, the Cu $2p_{3/2}$ line shape was unchanged by 30-Å Cr cluster assembly at $T\leq100$ K. The O $1s$ emission did broaden to higher binding energy and the Bi $4f$ emission showed a new (but small) component, as in Figs. 3 and 6. These results indicate substrate modification that was probably restricted to the terminal Bi-O layer.

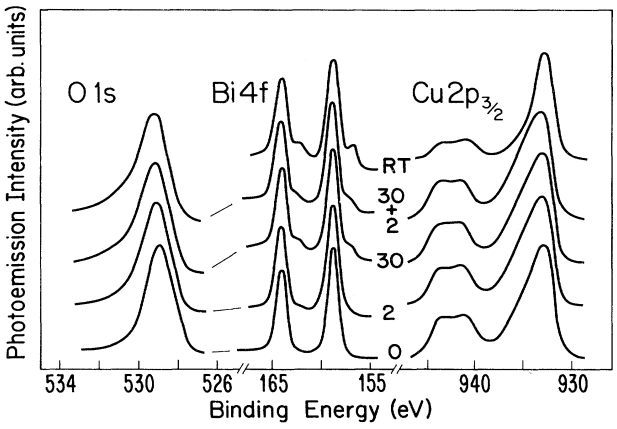

FIG. 7. Core-level emission EDC's for Cr(clusters) on $Bi_2Sr_2CaCu_2O_8$(100). The Cu $2p_{3/2}$ EDC's have been corrected for small contributions from condensed Xe, and a linear background has been subtracted. The appearance of a shoulder on the Bi $4f$ features indicate slight substrate disruption, and there is a small reduction of the Cu $2p_{3/2}$ satellite. The addition of 2-Å Cr as atoms at 20 K does not change the substrate line shapes, indicating that the surface was covered. Warming to 300 K led to further reaction at the buried interface but the amount was small compared to that seen for atom deposition.

Figure 5 shows the substrate attenuation for Cr clusters. The rate of attenuation is similar to a uniform layer for the first three cluster-assembly cycles, but the Cr clusters apparently coalesced at higher coverage. This behavior is consistent with the trends in γ, namely, $\gamma_{Cr}=2.3$ J/m^2, $\gamma_{Au}=1.5$ J/m^2, and $\gamma_{Ge}=1.0$ J/m^2 (Ref. 20). (Ge clusters did not delaminate and coalesce into large aggregates at 20 or 300 K, while Au clusters did at 300 K, but not 20 K.) Although surface diffusion would be slow at ~100 K, the amount of energy released by the formation of a Cr-Cr grain boundary, ~3.9 J/m^2, is considerably greater than for Au clusters. This very low temperature sintering in the presence of a substrate probably also gains from the small volume-surface ratio of the nanoclusters as the energy released is dissipated by a small volume. Despite this surface rearrangement of the clusters, the reactivity with the substrate is still very small.

The coalescence of the Cr clusters introduced some uncertainty as to whether the HTS surface was completely covered. This was tested by atom deposition of 2-Å Cr over the 30-Å cluster-assembled layer. The results shown in Fig. 7 reveal no substantial changes in the substrate EDC's. Figure 7 also shows the effect of subsequent warming to 300 K, namely, an increase in the low-binding-energy Bi emission, a reduction of the Cu satellite-to-main-line ratio to 60% of its clean-surface value, and a sharpening of the main line. The changes upon warming are greater than those observed for Ge clusters, but they are significantly less than for Cr atom deposition at 300 K. These results therefore provide another indication of the barrier formed by cluster deposition and the temperature dependence of the reaction pathway.

E. Interfacial reaction of Cu(clusters) on $Bi_2Sr_2CaCu_2O_8$(100)

The low heats of formation of CuO and Cu_2O ($\Delta H_f=-155$ and -166 kJ/mol, respectively) suggest the Cu overlayers might not result in the disruption observed for Ge and Cr, even for atom deposition. However, Hill *et al.*[10] reported disruption of both Bi-O and Cu-O planes and the conversion of substrate Cu from +2 to +1 upon deposition of small numbers of Cu atoms. Hence, we might expect the results for Cu cluster deposition to provide additional insight into surface processes where there are modest thermodynamic driving forces.

For Cu cluster deposition onto $Bi_2Sr_2CaCu_2O_8$(100), the emission intensity variations for O $1s$ and Bi $4f$ core levels follow the pattern established for Ge clusters in Fig. 5, namely, attenuation that is approximately the same as a uniform layer, as with Au and Ge clusters. There is no evidence of changes in the O $1s$ emission that would suggest reaction since the O $1s$ substrate feature at 528.8 eV did not shift or broaden. Likewise, no changes were observed in the Bi $4f$ line shape or peak position for depositions up to 20 Å. Intriguingly, however, the Cu $2p_{3/2}$ satellite was reduced much more rapidly than would be predicted for a growing nonreactive overlayer,

and this provides the evidence for Cu(clusters) on $Bi_2Sr_2CaCu_2O_8$ reaction. Indeed, the deposition of 2 Å of Cu reduced the satellite more than would be expected for reacting clusters decorating the surface as in Fig. 1. The satellite intensity was negligible by ~4 Å. It appears, therefore, that more complete wetting of the surface has occurred for Cu cluster deposition.

The observed reactivity following Cu cluster deposition suggests that the barrier formed was much less effective than for the other systems. Although the binding energy of the intermediate state of the activated process is not known for any overlayer, transfer of a Cu atom from the Cu cluster to the Cu-O-based HTS is equivalent to the formation of a Cu defect in the HTS, a relatively low-energy process. If this were the case, the intermediate state might not be energetically costly and it could explain the low-energy barrier.

Warming the 20-Å Cu(clusters) on $Bi_2Sr_2CaCu_2O_8$ interface to 300 K resulted in further roughening of the overlayer, as evidenced by an increase by ~20% of the Bi $4f$ substrate emission and a decrease by ~40% of the Cu $2p_{3/2}$ emission. This similarity to the Au cluster-assembled layer reflects the similar values for the surface free energies,[20] i.e., $\gamma_{Au}=1.5$ J/m^2 and $\gamma_{Cu}=1.8$ J/m^2. Warming also produced a new Bi $4f$ component because Bi atoms were released from the disrupted Bi-O plane by a Cu-$Bi_2Sr_2CaCu_2O_8$ reaction.[10]

F. Cluster assembly of Cr on $YBa_2Cu_3O_7$(100)

To generalize our results for cluster assembly on HTS surfaces, we investigated Cr cluster assembly on $YBa_2Cu_3O_7$(100). From atom deposition studies,[1] $YBa_2Cu_3O_7$ is less stable than $Bi_2Sr_2CaCu_2O_8$, probably because of self-passivation due to the Bi-O terminal planes. In Fig. 8, we show results for Cr(clusters) on $YBa_2Cu_3O_7$(100). The bottom curves for the clean surface[4] agree very well with those reported by Fowler *et al.*[33] for single-crystal surfaces, with sample-to-sample variations similar to what they discussed. The Cu $2p_{3/2}$ emission is typical of a +2 formal valence. The Ba $3d$ and $4d$ features are interesting because they show two spin-orbit-split features, with the high-binding-energy feature at 528.0 eV. Our best single-crystal results for cleavage at 20 K (or 300 K) had ~15% surface contamination based on the O $1s$ feature at 531 eV, probably due to inclusions formed during growth.

For Cr(clusters) on $YBa_2Cu_3O_7$(100), we formed clusters in 2-Å increments up to 14 Å. As shown in Fig. 8, the Cu $2p_{3/2}$ satellite-to-main-line ratio decreased to 60% of the clean value by 6-Å Cr cluster deposition while the main line sharpened, consistent with +2 to +1 conversion. The Ba $3d_{5/2}$ emission broadened as the high-binding-energy surface doublet was reduced, and additional intensity was added at higher binding energy because of a reacted feature. The O $1s$ EDC's (not shown) reveal a new component at ~531 eV due to Cr-O formation, and this contribution increased until ~6 Å. There were no changes in line shape for the substrate features after 8-Å Cr cluster deposition. This indicates that the reaction had been curtailed. The Cr $2p_{3/2}$ emission was characteristic of metallic Cr, although comparison to results for Cr(clusters) on $Bi_2Sr_2CaCu_2O_8$(100) suggested oxidation at the buried interface because there was additional intensity at higher binding energy.

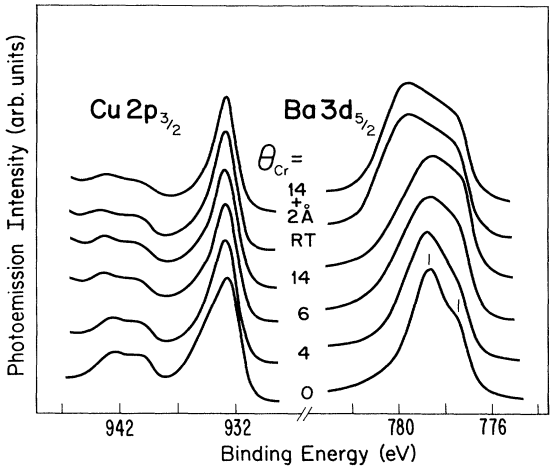

FIG. 8. Cu $2p_{3/2}$ and Ba $3d_{5/2}$ EDC's for Cr(clusters) on $YBa_2Cu_3O_7$(100). Cluster deposition results in partial loss of Cu $2p_{3/2}$ satellite emission and a small shift of the Ba $3d_{5/2}$ centroid. These changes are very small compared to atom deposition onto $YBa_2Cu_3O_7$. Even this reaction was curtailed by ~6-Å clusters. Warming to 300 K resulted in some additional reaction, as shown by an increase in the reacted Ba $3d_{5/2}$ component at ~780 eV and loss of Cu satellite emission. The addition of 2 Å of Cr atoms at 300 K produced no further changes because the overlayer was complete.

Warming to 300 K produced chemical changes at the interface, as is evident from the EDC's of Fig. 8. In particular, there was a shift and broadening of the Ba $3d_{5/2}$ emission because of conversion of the substrate component into the reacted-Ba component at ~780 eV. This reaction product is similar to that formed upon reactive atom deposition, as for Ti on $YBa_2Cu_3O_7$, but to a lesser extent.[2] Remarkably, the persistence of the Cu $2p_{3/2}$ satellite indicates that substantial amounts of Cu^{2+} remained in the probed area. There were no changes in the intensities of the various components that would indicate delamination. To rule out the possibility of contributions from uncovered areas, we deposited 2 Å of Cr as atoms at 300 K onto the cluster-assembled layer. As shown, there were no changes in the substrate emission. The significant amount of remaining Cu $2p_{3/2}$ satellite and the unmodified Ba $3d_{5/2}$ substrate emission demonstrate that Cr cluster deposition provides a method for forming relatively abrupt junctions with $YBa_2Cu_3O_7$, even for very reactive materials.

IV. SUMMARY

The formation of Au, Ge, Cu, and Cr overlayers by cluster assembly has been investigated for single-crystal

HTS substrates with XPS. TEM and STM structural studies have provided additional information concerning the way these nanoclusters interacted with the substrate and with each other. The observed overlayer reactivities and morphologies are consistent with trends in the bulk heats of oxide formation and surface free energies. They show minimal reaction on $Bi_2Sr_2CaCu_2O_8$ at temperatures below ~ 100 K. Warming to 300 K resulted in no changes for Au, limited reaction for Ge, and somewhat more reaction for Cr, in accordance with oxide heats of formation. Cr clusters aggregate at the low growth temperatures while Au showed aggregation at 300 K and Ge clusters remained uniformly spread, reflecting differences in the surface energy of the nanoclusters. The nanometer-sized clusters wetted silica and $Bi_2Sr_2CaCu_2O_8(100)$, and there was sintering at $T < 100$ K. Cu clusters on $Bi_2Sr_2CaCu_2O_8$ were reactive and showed the lowest barrier against reaction. These results demonstrate that the physical properties of the interface can be altered by cluster assembly.

ACKNOWLEDGMENTS

The authors wish to thank T. J. Wagener, J. C. Patrin, H. M. Meyer III, and G. D. Waddill for stimulating discussions concerning cluster assembly. This work was supported by the Office of Naval Research (Minnesota), by the National Science Foundation (Texas), and by Nippon Telegraph and Telephone Laboratories.

[1]See H. M. Meyer, III and J. H. Weaver, in *Physical Properties of High Temperature Superconductors II,* edited by D. M. Ginsberg (World-Scientific, Singapore, 1990), pp. 369–457, and extensive references therein.

[2]H. M. Meyer, III, D. M. Hill, T. J. Wagener, Y. Gao, J. H. Weaver, D. W. Capone II, and K. C. Goretta, Phys. Rev. B **38**, 6500 (1988).

[3]T. R. Ohno, J. C. Patrin, H. M. Meyer, III, J. H. Weaver, Y. Kimachi, and Y. Hidaka, Phys. Rev. B **41**, 11 677 (1990).

[4]H. M. Meyer, III, D. M. Hill, T. J. Wagener, J. H. Weaver, C. F. Gallo, and K. C. Goretta, J. Appl. Phys. **65**, 3130 (1989).

[5]T. R. Ohno, Y.-N. Yang, J. H. Weaver, Y. Kimachi, and Y. Hidaka, Appl. Phys. Lett. **57**, 718 (1990).

[6]D. M. Hill, H. M. Meyer, III, J. H. Weaver, and N. D. Spencer, Surf. Sci. **236**, 377 (1990).

[7]T. J. Wagener, Y. Gao, I. M. Vitomirov, C. M. Aldao, J. J. Joyce, C. Capasso, J. H. Weaver, and D. W. Capone, II, Phys. Rev. B **38**, 232 (1988).

[8]H. M. Meyer, III, T. J. Wagener, D. M. Hill, Y. Gao, S. G. Anderson, S. D. Krahn, J. H. Weaver, B. Flandermeyer, and D. W. Capone, II, Appl. Phys. Lett. **51**, 1118 (1987).

[9]D. S. Dessau, Z.-X. Shen, B. O. Wells, W. E. Spicer, R. S. List, A. J. Arko, R. J. Bartlett, Z. Fisk, S.-W. Cheong, D. B. Mitzi, A. Kapitulnik, and J. E. Schirber, Appl. Phys. Lett. **57**, 307 (1990).

[10]D. M. Hill, H. M. Meyer, III, J. H. Weaver, C. F. Gallo, and K. C. Goretta, Phys. Rev. B **38**, 11 331 (1988).

[11]C. T. Cheung and E. Ruckstein, J. Mater. Res. **4**, 1 (1989).

[12]R. S. Williams and S. Chaudhury, in *Chemistry of High Temperature Superconductors II,* edited by D. L. Nelson and T. F. George (American Chemical Society, Washington, D.C., 1988), pp. 291–302.

[13]G. D. Waddill, I. M. Vitomirov, C. M. Aldao, S. G. Anderson, C. Capasso, J. H. Weaver, and Z. Liliental-Weber, Phys. Rev. B **41**, 5293 (1990), and references therein. See also J. H. Weaver and G. D. Waddill, Science (to be published).

[14]I. M. Vitomirov, C. M. Aldao, G. D. Waddill, and J. H. Weaver, J. Vac. Sci. Technol. A **8**, 3368 (1990).

[15]R. E. Honig and H. O. Hook, RCA Rev. **21**, 360 (1960).

[16]Y. Hidaka and T. Murakami, Phase Transitions **15**, 241 (1989); Y. Hidaka, M. Oda, M. Suzuki, Y. Maeda, Y. Enomoto, and T. Murakami, Jpn. J. Appl. Phys. **27**, L538 (1988).

[17]R. Pretorius, J. M. Harris, and M.-A. Nicolet, Solid State Electron. **21**, 667 (1978).

[18]L. Kepinski, Thin Solid Films **78**, 133 (1981).

[19]E. B. Priestley and P. J. Call, Thin Solid Films **69**, 39 (1980).

[20]F. R. deBoer, R. Boom, W. C. M. Mattens, A. R. Miedema, and A. K. Niessen, *Cohesion in Metals* (North-Holland, New York, 1988), pp. 662–663.

[21]R. A. Swalin, *Thermodynamics of Solids* (Wiley, New York, 1972), pp. 220–257.

[22]P. G. de Gennes, Rev. Mod. Phys. **57**, 827 (1985).

[23]P. C. Wayner, Jr., J. Colloid Interface Sci. **88**, 294 (1982).

[24]J. Mahanty and B. W. Ninham, *Dispersion Forces* (Academic, New York, 1976); J. N. Israelachvili, *Intermolecular and Surface Forces* (Academic, New York, 1985).

[25]H. Krupp and G. Sperling, J. Appl. Phys. **37**, 4176 (1966).

[26]H. E. Exner and E. Arzt, in *Sintering Key Papers,* edited by S. Somiya and Y. Moriyoshi (Elsevier Science, New York, 1990), pp. 157–184.

[27]A. R. Tholen, in *Contributions of Cluster Physics to Materials Science and Technology,* edited by J. Davenas and P. M. Rabette (Martinus Nijhoff, Boston, 1986), pp. 601–615.

[28]J. H. Weaver, H. M. Meyer, III, T. J. Wagener, D. M. Hill, Y. Gao, D. Petersen, Z. Fisk, and A. J. Arko, Phys. Rev. B **38**, 4668 (1988).

[29]R. C. Jaklevic and L. Elie, Phys. Rev. Lett. **60**, 120 (1988).

[30]J. E. Castle and D. Epler, Proc. R. Soc. London, Ser. A **339**, 49 (1974).

[31]*CRC Handbook of Chemistry and Physics,* 57th ed., edited by R. C. Weast (CRC Press, Cleveland, 1976), pp. D69–71.

[32]I. Ikemoto, K. Ishii, S. Kinoshita, H. Kuroda, M. A. Alario Franco, and J. M. Thomas, J. Solid State Chem. **17**, 425 (1976); G. C. Allen, M. T. Curtis, A. J. Hooper, and P. M. Tucker, J. Chem. Soc. (Dalton) 1675 (1973).

[33]D. E. Fowler, C. E. Brundle, J. Lerczak, and F. Holtzberg, J. Elect. Spectros. Relat. Phenom. **52**, 323 (1990), and reference therein.

[34]C. C. Chang, M. S. Hegde, X. D. Wu, B. Dutta, A. Iman, J. Venkatesan, B. J. Wilkens, and J. B. Wachtman, Jr., Appl. Phys. Lett. **55**, 1680 (1989).

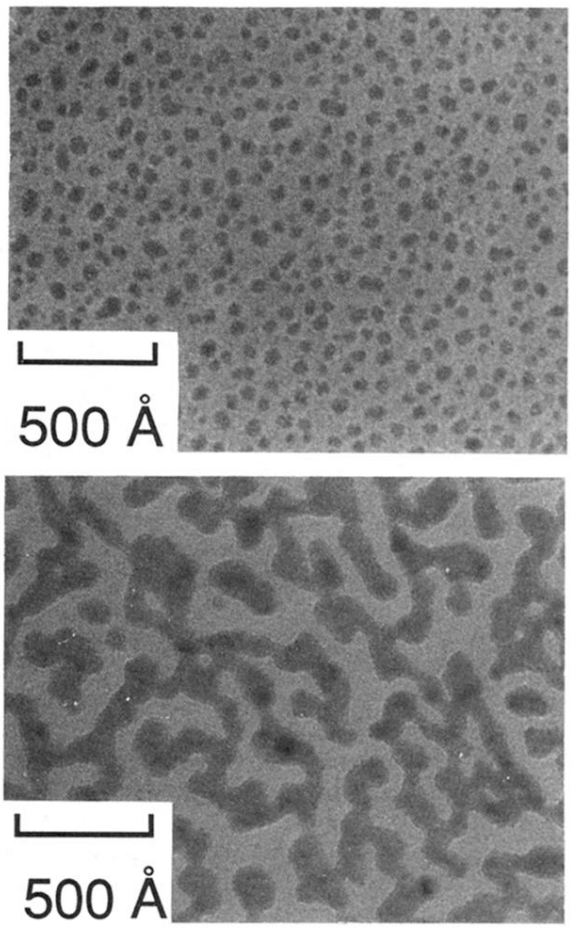

FIG. 1. TEM images of Cu cluster assembly on silica. The upper panel for 2-Å deposition shows irregular clusters over ~25% of the surface (characteristic diameter ~40 Å). The lower panel shows the structure obtained by three successive 2-Å cluster depositions. In this case, the interconnected Cu labyrinth covered ~60% of the surface (estimated thickness ~10 Å). The TEM images showed little contrast after ten such cluster depositions.

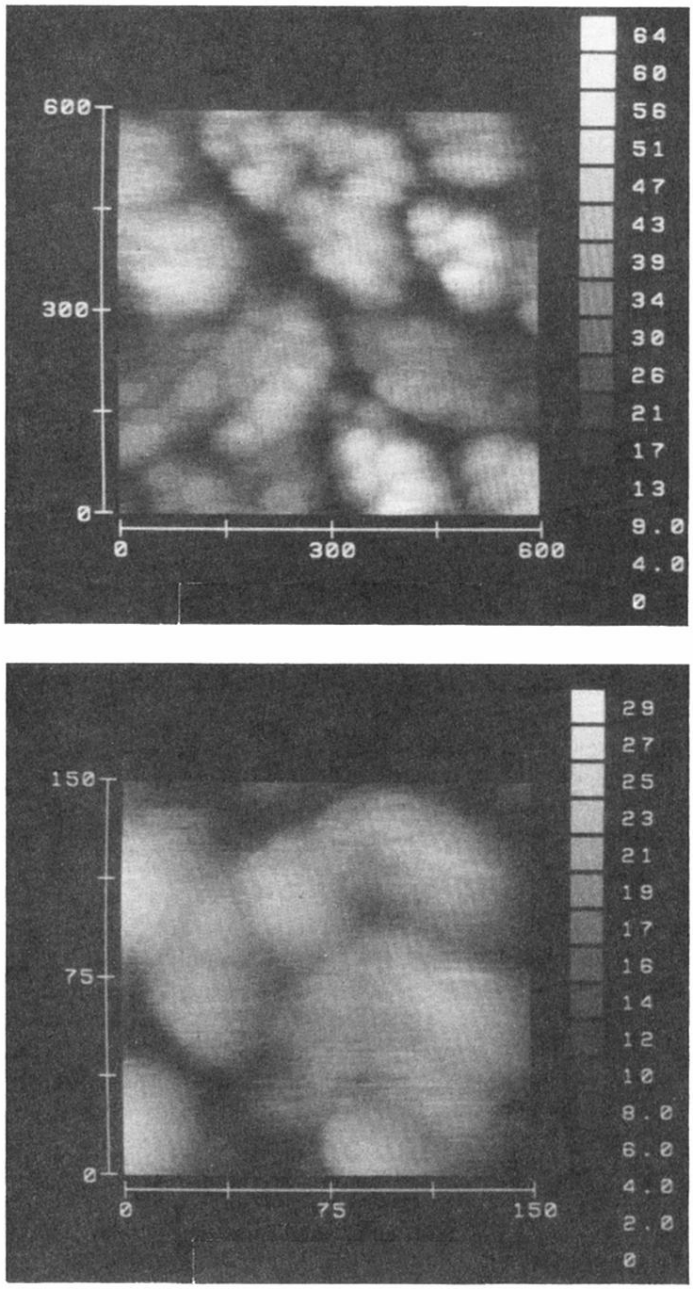

FIG. 2. STM images for 20-Å Au cluster assembly on $Bi_2Sr_2CaCu_2O_8$(100) after warming to 300 K and a brief air exposure. The upper image for a 600×600-Å^2 region taken with a -15-V tip bias and 100-pA tunneling current shows coarse patches with a typical dimension of ~150 Å and covering $\sim80\%$ of the surface. The dark regions reflect voids formed by cluster coalescence and delamination from the HTS surface. The lower image for a 150×150-Å^2 area (-1 V, 100 pA) shows a single patch that resembles an aggregate composed of smaller clusters of characteristic dimension ~30 Å. The calibrated gray scales on the right-hand side give an indication of height in Å.